Geodesy and Geodynamics 10 (2019) 297–306

Contents lists available at ScienceDirect

Geodesy and Geodynamics

journal homepage: http://www.keaipublishing.com/geog

Attenuation of coda waves in the SW of High-Atlas area, Morocco

Roumaissae Azguet [a, b, *], Ghizlane Bouskri [a], Youssef Timoulali [a], Mimoun Harnafi [a], Younes EL. Fellah [c]

[a] Scientific Institute, Mohamed V University in Rabat, Morocco
[b] Faculty of Science, Mohammed V University in Rabat, Morocco
[c] Rural Engineering Department, Institut agronomique et vétérinaire hassan II, Rabat, Morocco

ARTICLE INFO

Article history:
Received 16 January 2018
Accepted 7 May 2019
Available online 16 May 2019

Keywords:
Attenuation
Coda waves
Quality factor
Frequency
Souss basin
Morocco

ABSTRACT

We investigate attenuation scattering and loss properties in Souss basin (SW of High-Atlas) as a transition zone between the High and Anti Atlas ranges. This district consists in a thinned crustal patch with shallow seismicity and loose sedimentary trenches that perform an important contribution to augment seismic attenuation. So far, no coda waves approach in our knowledge have been used to draw satisfying outputs about the attenuation properties in the region. Therefore, this update suggests to correlate the lateral changes of seismic attenuation to different characteristics and asperities i.e. seismic activity, crustal age and thickness, heat flow, and ground deformation rate. To do so, we analysed coda waves derived from waveform data of more than 23 local earthquakes from seven broadband seismometers recorded during 2010–2012 period. As a starter, we utilized the backscattering model which defines the seismic attenuation as inversely proportional to quality factor by the equation $\left(A = {}^{1}/_{Q_c}\right)$. Q_c estimates were deducted at various central frequency bands 1.5, 3.0, 6.0, 9.0, 12.0 and 18.0 Hz according to different lapses times. The estimated average frequency dependence quality factor gives relation $Q_c = 120f^{1,01}$, while the average Q_c values vary from 149 at 1.5 Hz to 1895 at 18 Hz central frequencies. We observed an intimate dependence between quality factor and frequency ranges, which reflects the complexity of geological/geophysical pattern in the Souss basin and the presence of a variety of heterogeneities within the underlying crust.

© 2019 Institute of Seismology, China Earthquake Administration, etc. Production and hosting by Elsevier B.V. on behalf of KeAi Communications Co., Ltd. This is an open access article under the CC BY-NC-ND license (http://creativecommons.org/licenses/by-nc-nd/4.0/).

1. Introduction

Several studies extend their view on the Earth's system as being, in the best scenarios an isotropic and elastic medium. In contrast, attenuation studies deal particularly with anelasticity and anisotropy, which is one of the master components beyond leading seismic waves to decrease their amplitude. In general, attenuation is described by a drop-down in the energy level and signal amplitude of seismic waves due to their reflection and transmission within discrete interfaces [1]. This phenomenon is tackled by four parameters among which three are elastic and conserve the energy propagation wave field, e.g. geometrical spreading, scattering, and multipathing. The fourth effect is anelasticity which involves conversion of the seismic energy, and sometimes is also referred to as intrinsic attenuation, which controls in many ways seismic attenuation of coda and body waves [2,3]. In order to quantify the energy dissipation in a medium materialized by the amplitude decay on seismograms, a non-dimensional parameter has been brought to the surface called quality factor Q [4].

Anterior source models regarding seismic activity at the Atlas range exhibited the presence of moderate but complex earthquakes, which makes some conventional methods that aim at studying the energy decay modalities relatively erroneous and

* Corresponding author. Scientific Institute, Mohamed V University in Rabat, Morocco.
E-mail address: azguet.roumaissae@gmail.com (R. Azguet).

Peer review under responsibility of Institute of Seismology, China Earthquake Administration.

Production and Hosting by Elsevier on behalf of KeAi

https://doi.org/10.1016/j.geog.2019.05.001

1674-9847/© 2019 Institute of Seismology, China Earthquake Administration, etc. Production and hosting by Elsevier B.V. on behalf of KeAi Communications Co., Ltd. This is an open access article under the CC BY-NC-ND license (http://creativecommons.org/licenses/by-nc-nd/4.0/).

unworthy. Alternatively, coda waves confer more possibilities to examine the frequency-dependent amplitude decay for several reasons, i.e. being extended at sufficient decay envelops to study the amplitude decline, allowing to select different time windows to track time dependent attenuation changes and being independent to the number of stations used in the analysis.

The attenuation properties of several seismic regions around the world have been determined by a number of researchers [2,5–10]. Most of these studies have been accomplished using direct empirical estimation of coda waves quality factors, wherein the single backscattering model has been emphasized. Accordingly, numerous findings have put in evidence that Q_c values are strongly dependent to frequency [2,7–9,11,12].

In this paper, frequency-dependent Q_c was estimated for local earthquakes recorded in the seismically active transect located at the SW of High-Atlas i.e. Souss basin (Fig. 1). For the first time in Morocco, we suggest a different study of the attenuation pattern and its physical and tectonic properties in the High Atlas. Most of attenuation outputs concerning Morocco were carried in the northern part of Morocco [13–15]. Hence, this paper is a new contribution to the seismological research in Morocco with a specific focus on quality factor estimates that will be specific to Agadir region crustal area without significant biases. This paper argues the presence of deep structure beneath the study area.

2. Geological setting

The Souss basin (Fig. 1), of the Moroccan Western High Atlas takes part in the NW African passive margin [16]. Several research works have studied the basement of Souss basin [17–26]. The basin sediments were uplifted during the Oligocene, suggesting a regional Alpine orogenesis [27]. The basement corresponds to Precambrian metamorphic rocks that are unconformably overlain by folded Palaeozoic marine and continental sediments ofdata Late Cambrian–Carboniferous age [19]. Triassic trilogy is related to the initial rifting of the Atlantic Ocean and is present with red beds and evaporites that are locally associated with basaltic flows. Jurassic sequence consists in shallow marine carbonates and marginal-marine evaporites, followed by Cretaceous succession that contains mainly clastic deposits, deposited in a subsiding, E–W trending 'gulf-like' system [28,29]. Tertiary filling occupies coastal basins with extensive phosphatic deposits. The Agadir region occupies the Souss synclinal valley surrounded to the north by the High Atlas mountain and to the south by the Anti-Atlas range (Fig. 1). These chains have been created and uplifted during the Oligocene due to the convergence between Africa and Eurasia [30,31]. Tectonic activity is still on going in the Agadir region (Fig. 1), and corresponds to normal and strike-slip faults along the axis of High Atlas and through Agadir City [18].

3. Methods

Seismic coda results mainly from the scattering and diffraction of P and S waves when they propagate through multiscale asperities and discrepancies (e.g. faults, ruptures, velocity anomalies or densities, etc.) (Fig. 2), [2,5]. In general, seismic attenuation is related to frequency [32]:

$$Q_c(f) = Q_0 \cdot \left(\frac{f}{f_0}^n\right) \tag{1}$$

where $Q_c(f)$ is the frequency-dependent quality factor for coda wave, Q_0 is the reference quality factor value of Q_c at frequency f_0 (generally 1 Hz), and n is the frequency parameter that covariates heterogeneities from region to another and reflects the tectonic activity.

Coda waves were processed using the single back-scattering model developed by Aki and Chouet [2] for bandpass filtered seismograms at different narrow frequency bandwidths among the flat part of the frequency response e.g., 1.5, 3, 6, 9, 12 and 18 (Hz) to avoid signal distortion [2]. Seismograms with signal to noise ratio bellow 3 are discarded for quality issues. Only vertical components of seismograms were used and Q_c values were partially derived from the vertical component, followed by averaging and standard deviations computations in order to result with a final set of reliable quality factor estimates. The following equation explains the dependency of quality factors to central frequencies in the attenuation process, by considering different parameters to split the S-wave travel time that is half of the total elapsed duration [2]:

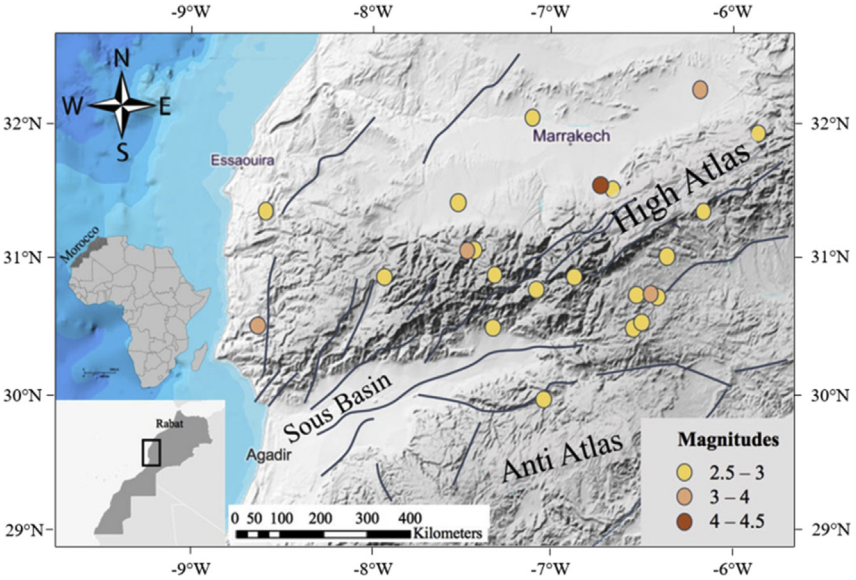

Fig. 1. Main: simplified neotectonic map with seismicity and active faults plot during 2010–2012 period. Top left: location of the Agadir region (SW High Atlas), study zone is bordered in bold.

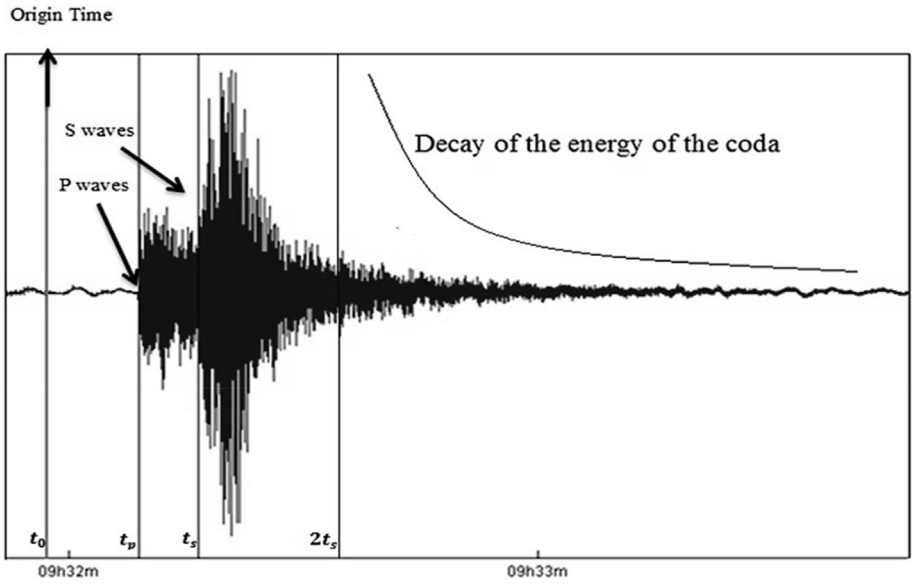

Fig. 2. Example of seismogram for the earthquake recorded on 17 November 2010 at 09:31:57 at the station MM12 with magnitude 3.1 showing the origin time, arrivals of P and S and the Coda.

$$A(f,t) = S(f)\, t^{-\beta} e^{-\pi f t/Q(f)} \tag{2}$$

where $S(f)$ is diffractive source factor at given frequency f, β is the geometrical spreading parameter. The formula relates the amplitude A of coda wave during a given lapse time t seconds from the origin time at a central frequency f to the quality factor Q_c. In general, coda is considered as a stack of scattered S-waves facing different heterogeneities located at different parts the crust and the upper mantle, accordingly to most of the theories, we will assume the geometrical spreading for body waves as $\beta = 1$ [33]. Taking the logarithm of Equation (2):

$$\ln(A(f,t)t) = \ln(S(f)) - \frac{\pi f t}{Q(f)} \tag{3}$$

Plotting the envelope of $ln(A(f,t)t)$ versus t at a given central frequency after band pass filtering the signal, gives a straight line with slope $=\frac{\pi f}{Q(f)}$ and hence $Q(f)$ can be determined. The calculation of $Q_c(f)$ from the RMS values of amplitude with time is shown in Fig. 3, along with the plot of the coda window selected. The single backscattering model allows calculating the depth of coda wave based on the Q_c value by considering a volume within the crust and lithosphere presumably an ellipsoid, with the following dimensions: $h = \frac{Vsta}{2}$, $l = \sqrt{h^2 - \frac{s^2}{4}}$ for equation (4):

$$E = l + d \tag{4}$$

where h and l represent the largest and the smallest axes of surface projection of the considered ellipsoid, E is lower border of the ellipsoid, V_s=3.55 km/s is the S-wave velocity, s refers to the distance made by the body wave from source to receiver, d is the earthquake depth, t_a=(t_{start}+$\frac{W}{2}$) is the average length of the time window which implies t_{start} as coda origin time in the seismogram with W as the total length of lapse time windows. In this study, we selected to use time lapses W of 40–60s, stepped with 10s. The variables we mentioned in this part allow tracking time and space dependent changes of coda attenuation by using them in equation (4).

Initially, Q_c values were computed using Coda Q MatLAB code [34] under SEISAN package [35]. However, we assume that the systematic use of conventional attenuation tools without consistent mathematical considerations can engender slightly biased results. Therefore, further linear regressions and empirical considerations were applied to obtain realistic estimates of Q_c, n and attenuation parameter, which allowed fitting resulting values to the regional geodynamical configuration of the Souss basin as a seismically active area.

4. Data

This investigation is based on seven broadband stations located upon different geological age. The Souss basin area consists of four stations (MM11, MM12, MM13, and MM14). One station (MB18) is deployed in the Anti-Atlas Mountains. Two of them are located in the High-Atlas domain (M204, MM15) (Fig. 4). All the equipment of temporary stations is homogeneous as explained in Table 1. We used *Taurus* digitizer as main recorder that performs under Linux, which is provided with a Nanometrics acquisition system with 50–100 samples/sec as a sampling rate and of frequency ranging between 50 and 100 Hz. The digitizer stores 1Go as maximum ground movement data volume in its IDE *hard* disk or flash memory CF Table 1. Seismic stations are equipped with Trillium 240 and STS2 seismometers characterized by their flat response to velocity from 240 s for 35 Hz from 100 s for 10 Hz, and have a self-noise level below the Low Noise Model (NLNM). These characteristics provide real-time information and allow detecting local and regional earthquakes as well as teleseisms.

Temporary stations were given a STS2 seismometer and high-resolution digitizer Quanterra Q330 data-loggers with 3–6 channels generally used for broadband frequencies, equipped with peripheral devices for external storage (hard disk or USB) (Table 1). Digitizers can be directly linked to *Seiscomp3* program for storage and they transfer synchronously to the recording process.

Concerning the dataset, we used 23 seismic events recorded during the 2010–2012 period, with depths smaller than 30 km and magnitudes ranging from 2.5 to 4.5.

5. Results and discussion

5.1. Frequency-dependent attenuation parameter

We got through the single backscattering model of Aki [2] to calculate the frequency-dependent attenuation parameters of coda

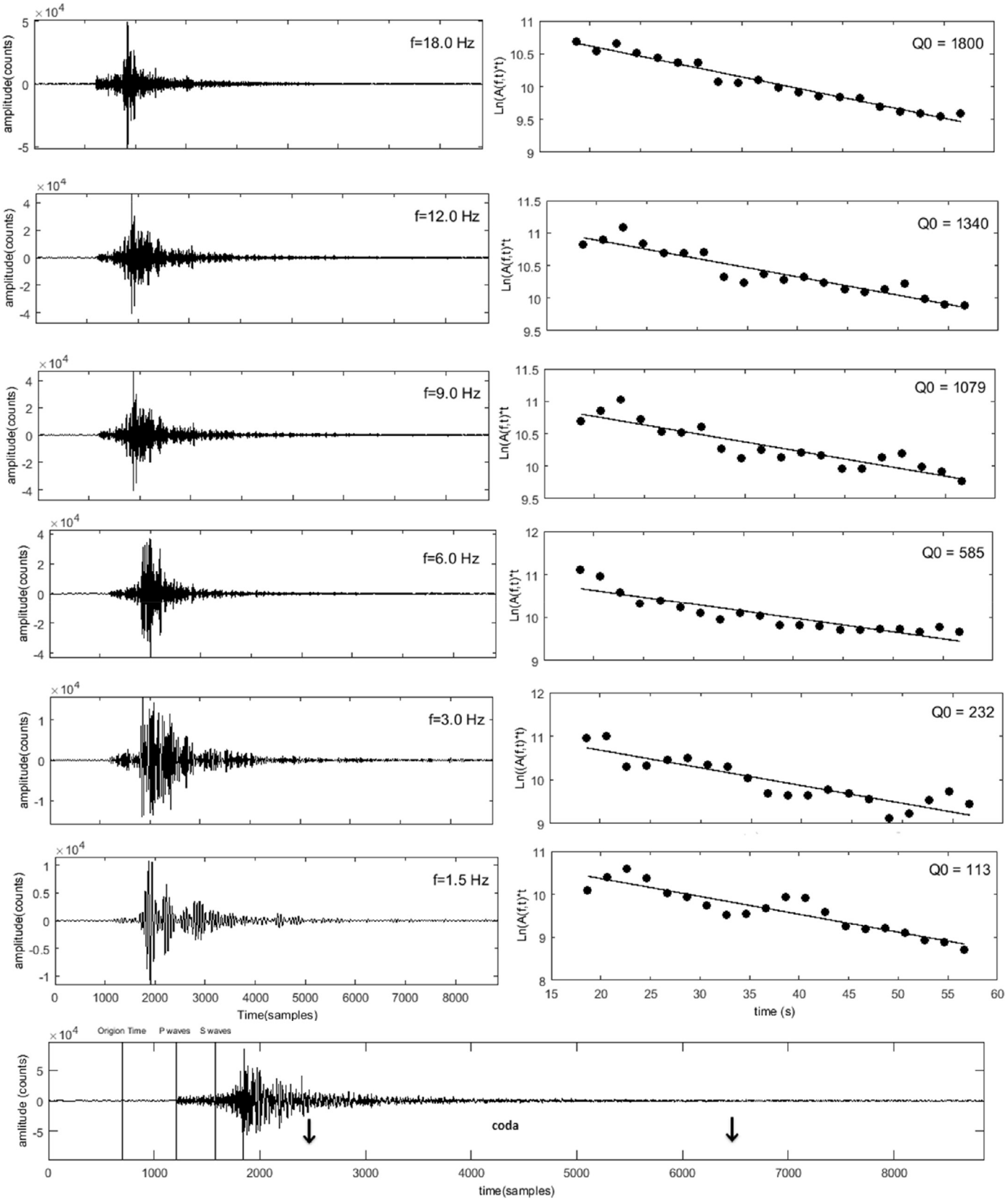

Fig. 3. Original (bottom) and band pass-filtered coda waves observed for a local earthquake recorded at MM11 station on 2010/11/17 at 09:31:57 with ML 3. The coda window length used for the Q_c estimation is indicated by arrows (left). Corrected and smoothed logarithmic coda amplitudes for the coda window are computed using the RMS technique. The straight line is fitted in a least square sense. The estimated Q_c value for each frequency component is also shown (right).

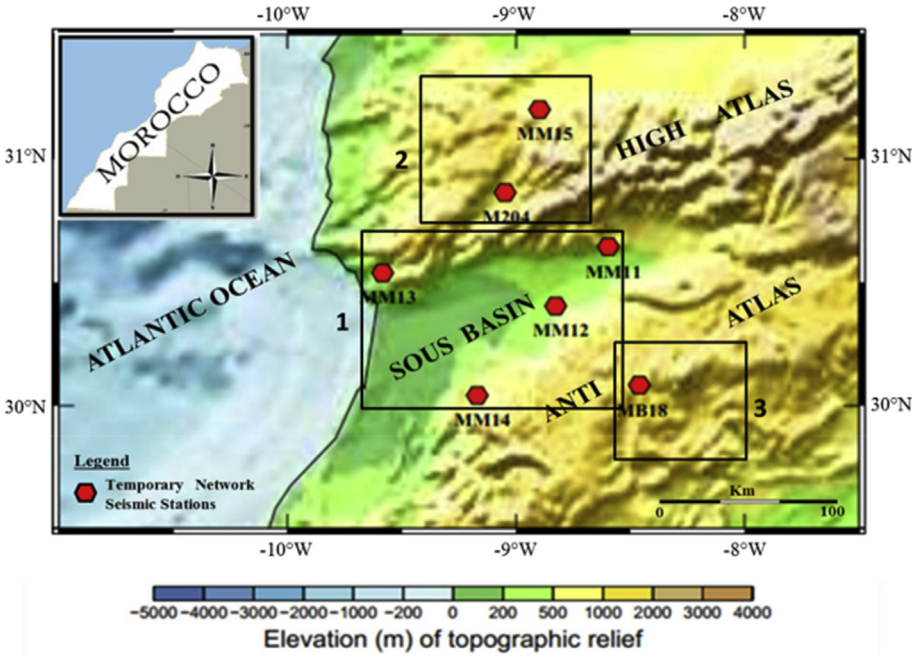

Fig. 4. Topographic map showing the temporary broadband stations deployed in the location of the study, The elevations (m) of the topographic relief are indicated on the colour scale, Rectangles 1, 2, and 3 are, Souss basin, High-Atlas, and Anti-Atlas regions, respectively.

Table 1
Characteristics of different permanent and temporary networks used in this study.

Network	Station	Station location	Number of components	Sensor type	Digitiser type	Communication	Lat. (°)	Long. (°)	Altitude (m)
Morocco-Array	MM11	Souss basin	3	Trillium 120	Taurus	Flash disk	30.6459	−8.5964	572.0
	MM12	Souss basin	3	Trillium 120	Taurus	Flash disk	30.4052	−8.8270	358.0
	MM13	Souss basin	3	Trillium 120	Taurus	Flash disk	30.5392	−9.5835	420.0
	MM14	Souss basin	3	Trillium 120	Taurus	Flash disk	30.0424	−9.1694	774.0
	MM15	High-Atlas	3	Trillium 120	Taurus	Flash disk	31.1991	−8.8973	955.0
Topo-Iberia	M204	High-Atlas	3	Trillium 120	Taurus	Flash disk	30.8646	−9.0471	953.7
Bristol	MB18	Anti-Atlas	3	Trillium 120	Taurus	Flash disk	30.0840	−8.4603	1736.0

waves off the SW of High-Atlas. Among the central frequencies, seismograms have been analysed and were filtered using a 6-pole Butterworth filter at six bands 1.5, 3, 6, 9, 12 and 18 Hz according to 40, 50, and 60-s-duration lapse time windows starting from t = 2ts. Table 2 lists the estimates of Q_c with their standard deviations at different stations, and average values for the Souss basin region for three lapse

Table 2
Quality factor estimates values for different lapse times from the seven stations and for the whole study zone.

	Stations							
fc (Hz)	MM11	MM12	MM13	MM14	MM15	MB18	M204	The whole study zone
	(Q_c + *SD*)							
t_L = 40s								
1,5	132,8 ± 32,6	155,2 ± 49,2	140,5 ± 47,0	179,5 ± 38,8	147 ± 4,2	240,6 ± 92,9	196 ± 41,2	149,5 ± 41,7
3	319,5 ± 95,1	314,6 ± 56,5	268,7 ± 69,5	388,2 ± 143,1	375,6 ± 138,9	456,2 ± 59,0	609 ± 121,2	423,8 ± 182,4
6	704 ± 173,8	712,3 ± 114,9	731,8 ± 264,5	839 ± 196,6	919,1 ± 314,0	1051,6 ± 152,3	865,1 ± 127,5	884,2 ± 261,8
9	1224,2 ± 178,5	1001,5 ± 152,9	992 ± 236,5	991,8 ± 188,6	1377,1 ± 436,4	1411,6 ± 214,9	1109,1 ± 203,9	1209,8 ± 221,2
12	1637,2 ± 351,4	1221,7 ± 169,9	1197,2 ± 237,5	1238,2 ± 227,4	1650,4 ± 335,2	1783,1 ± 280,9	1360,3 ± 188,4	1477,2 ± 282,5
18	2041,2 ± 318,9	1702,3 ± 156,4	1747,6 ± 250,9	1709,4 ± 200,4	2005,5 ± 246,6	2343,8 ± 542,1	1796,5 ± 263,2	1895,8 ± 231,4
t_L = 50s								
1,5	136 ± 20,8	180,4 ± 46,4	142 ± 41,0	–	150 ± 0	247 ± 58,5	220 ± 35,3	157,2 ± 40,6
3	432,5 ± 125,3	429,3 ± 93,9	440 ± 285,8	544,5 ± 86,8	422,2 ± 165,5	610,4 ± 147,5	764 ± 24,0	452,2 ± 145,4
6	982,1 ± 167,4	850,3 ± 91,0	862,4 ± 265,5	893 ± 103,8	1172 ± 322,4	1079,2 ± 208,5	1118 ± 321,4	896,7 ± 166,9
9	1401,1 ± 157,9	1171 ± 112,8	1091 ± 221,4	1106,5 ± 114,5	1581,5 ± 522,8	1508,5 ± 129,6	1317,8 ± 280,7	1230,2 ± 160,8
12	1687,4 ± 206,6	1440,6 ± 136,9	1344,2 ± 214,2	1406,5 ± 142,4	1910,3 ± 480,4	1697,2 ± 119,3	1593,5 ± 221,9	1536,3 ± 174,1
18	2136 ± 345,4	1783,2 ± 143,8	1954,8 ± 326,7	1832,8 ± 120,7	2433,4 ± 636,1	2128,7 ± 164,4	1961,6 ± 257,8	1908,4 ± 265,2
t_L = 60s								
1,5	199,6 ± 104,6	189,3 ± 29,5	262 ± 0	–	–	280 ± 0	269,3 ± 56,2	203,1 ± 78,7
3	494,5 ± 189,6	542,8 ± 81,6	522 ± 166,2	639,5 ± 121,3	410 ± 0	721,3 ± 141,7	895 ± 0	514,0 ± 132,1
6	1071,3 ± 131,9	1075,2 ± 87,6	1037,25 ± 236,8	1035,6 ± 243,4	1523,5 ± 248,2	1155,8 ± 231,6	1231,5 ± 294,2	1065,5 ± 133,2
9	1508,3 ± 50,9	1350,1 ± 89,4	1258,6 ± 189,0	1267,4 ± 183,9	1798,1 ± 247,2	1560,1 ± 170,2	1567,7 ± 251,3	1376,0 ± 147,4
12	1755,3 ± 153,8	1554,1 ± 96,6	1541,6 ± 127,3	1533,3 ± 197,5	2026,8 ± 365,7	1710,5 ± 134,6	1709,5 ± 246,6	1614,3 ± 153,3
18	2236,5 ± 308,3	1885,2 ± 132,4	2414 ± 342,7	1924 ± 139,1	2491,8 ± 705,8	2173,8 ± 174,2	2299,1 ± 450,2	2135,3 ± 334,8

time windows at different central frequencies. The overall average Q_c values, along with standard deviation, fluctuate between 149 ± 41, 157 ± 40, and 203 ± 78 at 1.5 Hz to 1895 ± 231, 1908 ± 265, and 2135 ± 334 at 18 Hz for lapse time windows of 40, 50, and 60 s, respectively (Table 2). We confirm then that the Q_c value increases with an increase of frequency as well as lapse time window.

The high attenuation (the low Q_c values) at the lower frequencies can potentially reflect a high loss rate of energy levels due to the presence of more heterogeneities than the rock can withstand. In contrary, the low attenuation (the high Q_c values) at higher frequencies exhibits the presence of less heterogeneities at the deeper parts of the upper crust [2]. In the same context, the average relationships for the entire region are set as Q_c=(120 ± 1,18) $f^{(1,01\pm0,08)}$, Q_c=(129 ± 1,18) $f^{(0,98\pm0,05)}$, Q_c=(165 ± 1,16) $f^{(0,93\pm0,07)}$ for lapse time windows of 40, 50, and 60 s, respectively. Several findings are consistent with a strong correlation between degree of frequency dependence and tectonic activity rate, and observed that n value is higher for tectonically active regions compared to regions of more stable pattern [7,36–39]. The sharp dependence relationship of Q_c to frequency can probably tell us more about the size of heterogeneities that are randomly distributed among the lithosphere [5]. P-wave tomography studies projected to the region [40] indicate the presence of high velocity anomalies in the south of Agadir crustal area between 5 and 45 km depth with P velocity ranging from 6.6 to 7.8 km/s. This crustal anomaly has been interpreted as an upper crustal brittle body that marks the edge-cutting limit between the Atlas domains in the north and the Anti-Atlas domain in the south.

Table 3 show the inferred Q_0 and n values for all selected lapse times. Q_0 estimates indicate a strong heterogeneity of the Souss basin and enrol the area under the tectonically active regions category. As shown in the frequency function plotted in (Fig. 5), these estimates are unambiguously increasing with frequency for all broadband stations over the entire region. Conversely. The n value decreases with the increase of Q_0 in a low frequency range, which is probably related to the tender sedimentary trench beneath the Souss basin or due to an important heat flow or a dense tectonic network within the crust. On the other hand, the n estimates become more coherent when placed in higher frequency ranges, which we assume to be relevant to the spread-off of backscattered body shear waves in deeper sections in the upper crust, being more homogeneous medium and therefore imposing less asperities [2].

5.2. Lapse time-dependent attenuation

The lapse time dependence in seismic attenuation is characterized by an increase in Q_0 and a decrease in frequency parameter n. In other words, the increase of Q_c with lapse time and systematically depth engenders an increase in Q_0 and a decrease in n [8]. This means that larger lapse times and Q_0 imply deeper parts of the crust and mantle where less heterogeneities subsist, and therefore less energy loss [7,41–44]. The comparative approach we built between Q_0 and n for each station deployed in this study (Fig. 6) is consistent with this theory and displays an increase of Q_0 (Fig. 6a) concomitant with a decrease in n with the lapse times (Fig. 6b). We deem that the results in (Fig. 6a, b) indicate that the lower part of the crust and the upper mantle contain an important amount of heterogeneities e.g. an important heat flow, seismogenic pattern, dense rupture networks. For instance, the Souss area around station MM11 is characterized by the lowest Q_0 and highest n and therefore attenuation pattern (Fig. 6; Table 3) in comparison to others stations, which is potentially due to a relatively thinner crust and more abundant seismic activity.

Fig. 7, exhibits increasing average Q_0 and Q_c and decreasing n values for the entire study region with an increase in time lapses. These findings are analogous to features observed in other tectonically active regions [7,39,41,43–48] and imply that attenuation decreases (Fig. 7b) with increasing depth and that deeper spots can be targeted by larger sampled coda lapse time windows.

Hence the increase in Q_c with the lapse time suggests that the deeper part of the study region is less heterogeneous than the shallower part. For instance, the sampled depth is less manifested at 40 s lapse time that at 50 and 60s. This may be related to the increasing cohesion and compaction coefficients of rocks with increasing geothermal gradient in depth. As a result, the seismic attenuation ($^1/_{Q_c}$) (Fig. 8) decreases along with particle motion with the increasing depth [49]. Confirmation of these observations is drawn by geological data and tomographic studies [40] that put in evidence the existence of high velocity anomaly body underlying the local structures beneath the Souss basin.

The comparison of the Coda Q results of the Souss basin region with the High Atlas and Anti-Atlas regions (Fig. 9) shows that the lowest values of Q_0 (Fig. 9a) and the highest values of n (Fig. 9b) were related to the Souss basin area, these results suggest that the crust in this area appears to be more 'attenuating' and heterogeneous. Our results are approved by the findings of receiver function analysis implied an interface at ~2 km depth that is more pronounced beneath the Souss basin and might be associated with sediments. Moreover, the Vp/Vs ratios beneath the basins exceed the value of 1.8 which might be related to the presence of marine sediments [50].

5.3. Comparison of results with other regions

The comparison results of attenuation parameters for different tectonic settings have shown that. Firstly, tectonically active areas are characterized by low Q_0 values ($Q_0 < 200$) and high values of frequency-dependent power ($n > 0.8$) [2,41,45,47,51–60]. Secondly, inactive tectonic regions are characterized by high Q_0 values ($Q_0 > 600$) and low values of frequency-dependent power ($n < 0.5$) [3,61–64]. Finally, moderate values of Q_0 and n ($200 < Q_0 < 600$,

Table 3
Average quality factor and n value estimates for different lapse times for whole study region($Q_0 \pm \sigma_{Q_0}$).

	Stations							
	MM11	MM12	MM13	MM14	MM15	MB18	M204	Average of the Souss basin area
t_L(s)	($Q_0 \pm \sigma_{Q_0}$)							
40	90,51 ± 1,11	96,75 ± 1,15	94,37 ± 1,06	138,96 ± 1,06	110,07 ± 1,19	170,47 ± 1,09	180,00 ± 1,22	120,72 ± 1,18
50	110,78 ± 1,23	143,5 ± 1,14	117,8 ± 1,09	261,72 ± 1,04	114,44 ± 1,23	207,30 ± 1,16	218,89 ± 1,29	129,46 ± 1,18
60	157,63 ± 1,16	164,02 ± 1,11	195,01 ± 1,08	371,14 ± 1,06	185,23 ± 1,61	248,09 ± 1,18	285,25 ± 1,24	165,05 ± 1,16
	($n \pm \sigma_n$)							
40	1,13 ± 0,05	1,02 ± 0,07	1,04 ± 0,05	0,89 ± 0,05	1,08 ± 0,08	0,94 ± 0,04	0,83 ± 0,10	1,01 ± 0,08
50	1,10 ± 0,10	0,92 ± 0,06	1,01 ± 0,09	0,67 ± 0,01	1,04 ± 0,10	0,85 ± 0,07	0,81 ± 0,13	0,98 ± 0,05
60	0,97 ± 0,07	0,91 ± 0,10	0,86 ± 0,04	0,56 ± 0,01	0,97 ± 0,21	0,79 ± 0,08	0,75 ± 0,10	0,93±,0,07

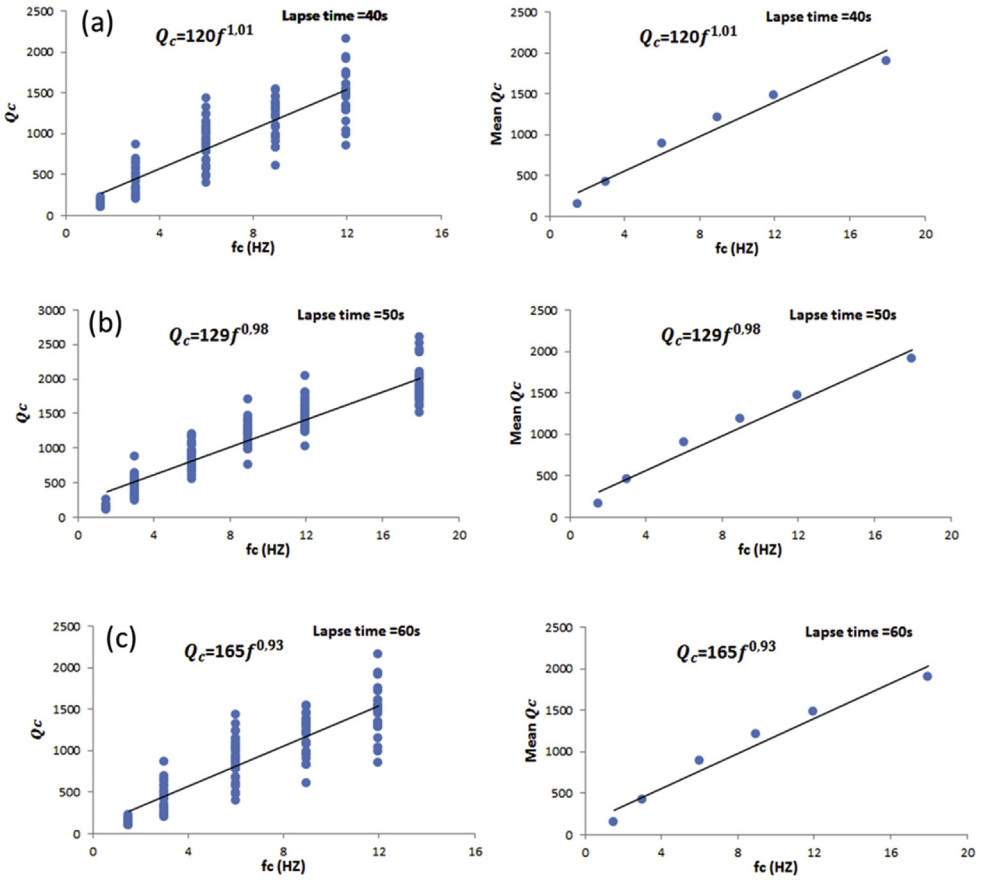

Fig. 5. Plot of $Q_c(f)$ and mean $Q_c(f)$ for the whole area, with linear regression frequency dependent relationship, $Q_c = Q_0 f^n$ at different lapse time. (a) lapse time = 40 s (b); lapse time = 50s; (c) lapse time = 60s.

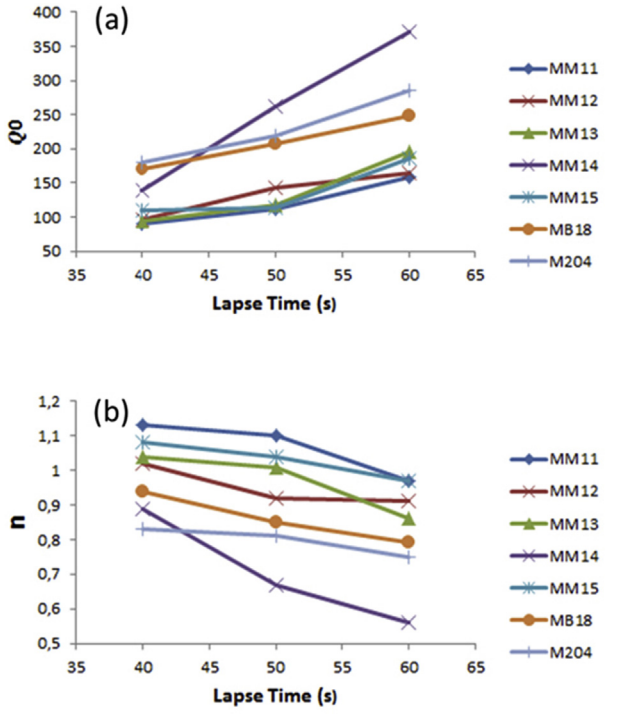

Fig. 6. (a) Plots of Q_0 with lapse time for all the stations (b) Plots of frequency parameter n with lapse time for all the stations.

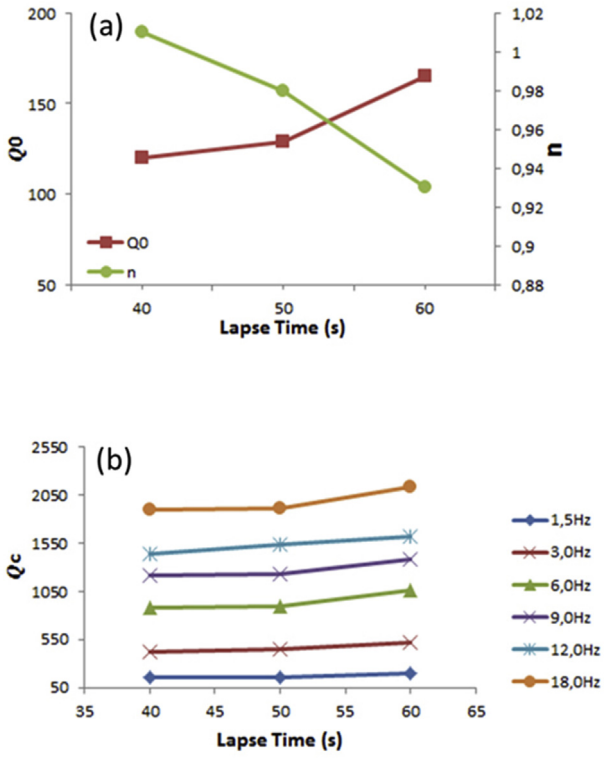

Fig. 7. Plot of average values of Q_c, Q_0 and n with lapse time for the Sous basin region. (a) Average Q_0 and n with lapse time (b) Average Q_c with lapse time at different central frequencies.

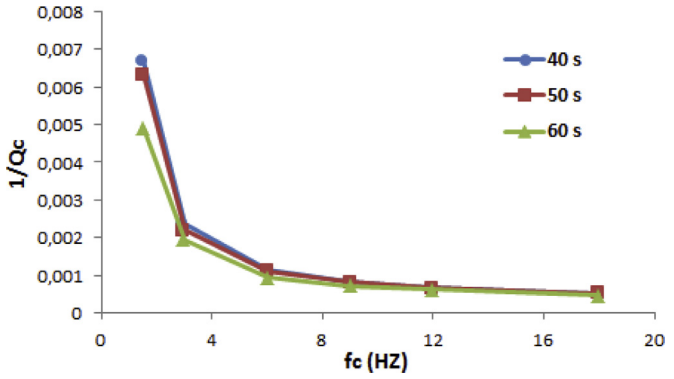

Fig. 8. A plot showing comparison of coda-*Qc* estimates for the Souss basin region, for different lapse time.

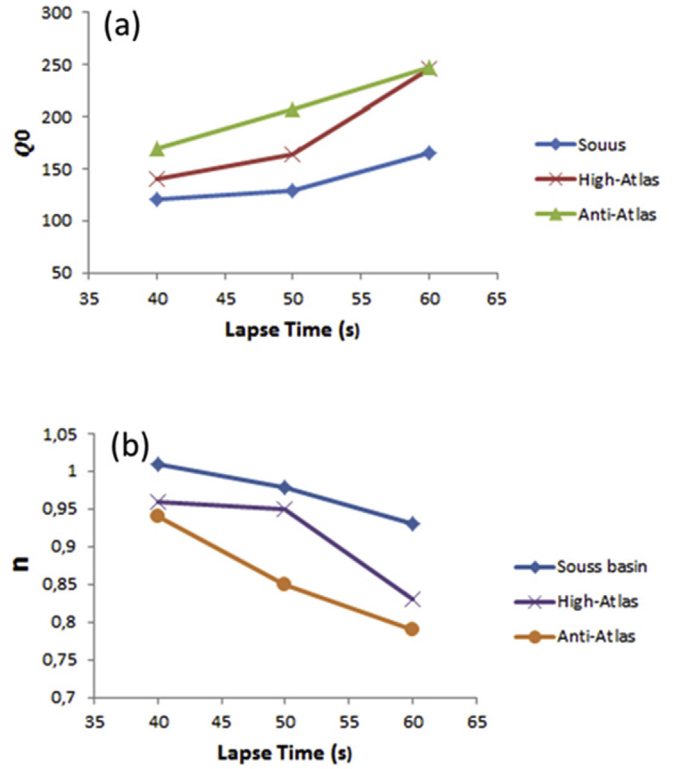

Fig. 9. Plot showing comparison of coda Q estimate of Souss basin, with High, and Anti Atlas area. (a) Plots of Q_0 with lapse times for three regions (b) Plots of n with lapse time for three regions.

$0{,}4 < n < 0{,}7$) obtained for regions between active and inactive areas are considered to be moderately active regions [7,8,65,66].

The average relationship for the entire region is set as $Q_c = 120f^{(1{,}01)}$. Our results generally show low Q_0 values (less than 200) for tectonically and seismically active regions. They are compatible with the Garhwal Himalayan $Q_c = 126f^{(0{,}95)}$ suggested by reference [50] and with the Garhwal–Kumaun Himalaya $Q_c = 119f^{(0{,}99)}$ reported by reference [54]. Table 4 presents Q_0 and n values for the selected studies.

Table 4
Parameters of the coda quality factor functions for different regions in the World.

Seismicity	Region	Q_0	n	Source
Active	Washington, United States	63	0.97	[45]
Active	Parkfield, California, United States	79	0.74	[51]
Active	Zagros, Iran	88	0.90	[53]
Active	Charlevoix, Quebec, Canada	91	0.95	[41]
Active	the Garhwal–Kumaun Himalaya	119	0.99	[54]
Active	this study	120	1,01	–
Active	the Garhwal Himalaya	126	0.95	[47]
Moderate	New England, United States	460	0.40	[8]
Moderate	South Indian Peninsular Shield	535	0.59	[65]
Moderate	New Madrid	598	0.54	[66]
Stable	NW Iberia	600	0,45	[62]
Stable	Northeast United States	900	0,35	[3]
Stable	Central United States	1000	0,20	[3]

6. Conclusion

We suggest, for the first time, a profound attenuation enquiry at the western high and anti-atlas bordure using the analysis of wave coda amplitude motion to retrieve quality factor Q_c that is associated to frequency by linear regression of the equation $Q_c = Q_0 f^n$. We processed 23 seismic events during the 2010–2012 periods recorded by seven broadband stations covering the Anti and the High Atlas Mountains. We used lapse times of 40s, 50s and 60s to derive 1) Coda time windows, 2) highlighting the high impact of multiple parameters, 3) signal noise related to different settings (season variations, depth of seismic station burial, proximity to the Atlantic offshore which is the case for the stations located in the west of Souss basin), 4) tectonic stability (generating medium to high frequencies of the Coda-Q estimates), 5) sedimentary layers trench, 6) the overall crustal structure. The frequency-dependent attenuation relations developed in the present study would be useful in various scientific and engineering applications, including earthquake hazard assessment, earthquake source parameter estimation, and understanding the physical phenomenon related to earthquake elastic energy propagation of the Agadir region, whereof further investigations are needed to correlate these results with seismic moment estimates and heat flow study in order to accurately speculate the origin of this discordance.

Conflicts of interest

The authors declare that there is no conflicts of interest.

Acknowledgement

The authors thank warmly anonymous reviewers for providing instructive comments and suggestions to enhance the scientific quality of this manuscript.

This study was supported by the Scientific Institute, Rabat, Morocco. Seismograms were supplemented from seismic stations that belong to the Morocco Array, Topo-Iberia and Bristol Networks, which had been set and installed in collaboration between the Scientific Institute, Mohammed V University in Morocco, Munster University in Germany, Bristol University and the Institute of Earth Sciences Jaume Almera.

References

[1] S. Stein, M. Wysession, An Introduction to Seismology, Earthquakes, and Earth Structure, Blackwell Publishing, 2003.

[2] K. Aki, B. Chouet, Origin of coda waves: source, attenuation, and scattering effects, J. Geophys. Res. 80 (23) (1975) 3322–3342.
[3] S. Singh, R.B. Herrmann, Regionalization of crustal coda Q in the continental United States, J. Geophys. Res. Solid Earth 88 (B1) (1983) 527–538.
[4] L. Knopoff, L.D. Porter, Attenuation of surface waves in a granular material, J. Geophys. Res. 68 (23) (1963) 6317–6321.
[5] K. Aki, Analysis of the seismic coda of local earthquakes as scattered waves, J. Geophys. Res. 74 (2) (1969) 615–631.
[6] H. Sato, Energy propagation including scattering effects sengle isotropic scattering approximation, J. Phys. Earth 25 (1) (1977) 27–41.
[7] S.W. Roecker, B. Tucker, J. King, D. Hatzfeld, Estimates of Q in central Asia as a function of frequency and depth using the coda of locally recorded earthquakes, Bull. Seismol. Soc. Am. 72 (1) (1982) 129–149.
[8] J.J. Pulli, Attenuation of coda waves in new England, Bull. Seismol. Soc. Am. 74 (4) (1984) 1149–1166.
[9] A. Jin, K. Aki, Temporal change in coda Q before the Tangshan earthquake of 1976 and the Haicheng earthquake of 1975, J. Geophys. Res. Solid Earth 91 (B1) (1986) 665–673.
[10] K.Y. Nishigami, Y. Ito, C. Gurbuz, A. Pinar, N. Aybey, S.B. Ucer, Y. Honkura, A.M. Iisikara, Microseismic activity and spatial distribution of coda-Q in the westernmost part of the north anatolian fault zone Turkey, Bull. Disaster Prev. Res. Inst. 40 (2) (1990) 41–56.
[11] T.G. Rautian, V.I. Khalturin, The use of the coda for determination of the earthquake source spectrum, Bull. Seismol. Soc. Am. 68 (4) (1978) 923–948.
[12] M. Tsujiura, Spectral analysis of the coda waves from local earthquakes, Bull. Earthq. Res. Inst. 53 (1978) 1–48.
[13] J. Xie, B.J. Mitchell, A back-projection method for imaging large-scale lateral variations of coda Q with application to continental Africa, Geophys. J. Int. 100 (2) (1990) 161–181.
[14] A. Boulanouar, L. El Moudnib, M. Harnafi, T.E. Cherkaoui, A. Rahmouni, M. Boukalouch, J. Sebbani, Spatial variation of coda wave attenuation using aftershocks of the Al Hoceima earthquake of 24 February 2004, Morocco, Nat. Sci. 5 (08) (2013) 72.
[15] M.J. Bezada, Insights into the lithospheric architecture of Iberia and Morocco from teleseismic body-wave attenuation, Earth Planet. Sci. Lett. 478 (2017) 14–26.
[16] J. Stets, P. Wurster, Atlas and Atlantic—structural relations, in: Geology of the Northwest African Continental Margin, Springer, Berlin. Heidelberg, 1982, pp. 69–85.
[17] A.E. Adams, D.V. Ager, A.G. Harding, Géologie de la région d'Imouzzer des Ida-ou-Tanane (Haut Atlas Occidental), Notes et Mém. Serv. géol. Maroc 41 (285) (1980) 59–80.
[18] R. Ambroggi, Etude géologique du versant méridional du Haut Atlas Occidental et de la plaine Souss, Notes et Mém. Serv. Géol. Maroc 157 (1963) 321.
[19] G. Choubert, A. Faure-Muret, Evolution du domaine atlasique marocain depuis les temps paléozoïques, Livre à la mémoire du Professeur Paul Fallot 1 (1962) 447–527.
[20] F. Duffaud, L. Brun, B. Plauchut, Le bassin du Sud-Ouest marocain, in: D. Reyre (Ed.), Bassins sédimentaires du littoral africain. Symp. New Delhi, Publ. Assoc. Serv. géol. Afr., Paris, I, 1966, pp. 5–26.
[21] G. Ercilla, J.I. Díaz, B. Alonso, M. Farran, Late Pleistocene-Holocene sedimentary evolution of the northern Catalonia continental shelf (northwestern Mediterranean Sea), Cont. Shelf Res. 15 (11–12) (1995) 1435–1451.
[22] B. Alonso, Gemma Ercilla Zárraga, F. Pérez, Estratigrafía sísmica del margen continental distal de Agadir y llanura abisal de Agadir: Retrogradación de un sistema turbidítico activo, in: XIII Congreso Espanol de Sedimentología, 1994, pp. 97–98.
[23] J. Rey, K. Tajeddine, M. Aadjour, B. Andreu, M. Adutem, R.K. Ben Abbas Taarji, M. Billotte, J. Canerot, N. El Kamali, E.M. Ettachfini, M. Ettachfini, A. Gharib, M. Ibnoussina, A. Rossi, O. Witam, Le Crétacé inférieur et moyen du Haut Atlas Occidental: Essai de synthes, Intern, in: Assoc. Sedimentology, 14th Regional Meeting, Marrakech, 1993, pp. 27–29.
[24] J. Wiedmann, A. Butt, G. Einsele, Cretaceous stratigraphy, environment, and subsidence history at the Moroccan continental margin, in: Geology of the Northwest African Continental Margin, Springer, Berlin. Heidelberg, 1982, pp. 366–395.
[25] O. Witam, J. Rey, M. Aadjour, J.F. Magniez, G. Delanoy, Nouvelles données biostratigraphiques et séquentielles sur la série barrémienne et aptienne du bassin d'Agadir (Maroc), Rev. Paléobiol. 12 (193) (1993) 202.
[26] A. Butt, Micropaleontological bathymetry of the cretaceous of western Morocco, Palaeogeogr. Palaeoclimatol. Palaeoecol. 37 (2–4) (1982) 235–275.
[27] A. Michard, Eléments de géologie marocaine, Notes et Memoires. Service géologique du Maroc 252 (1976) 1–422.
[28] M. Behrens, A. Siehl, Sedimentation in the atlas gulf I: lower cretaceous clastics, in: Geology of the Northwest African Continental Margin, Springer, Berlin. Heidelberg, 1982, pp. 427–438.
[29] P. Wurster, J. Stets, Sedimentation in the atlas gulf II: mid-cretaceous events, in: Geology of the Northwest African Continental Margin, Springer, Berlin. Heidelberg, 1982, pp. 439–458.
[30] E. Uchupi, K.O. Emery, C.O. Bowin, J.D. Phillips, Continental margin off western Africa: Senegal to Portugal, AAPG Bull. 60 (5) (1976) 809–878.
[31] P. Giese, V. Jacobshagen, Inversion tectonics of intracontinental ranges: high and middle atlas, Morocco, Geol. Rundsch. 81 (1) (1992) 249–259.
[32] B.J. Mitchell, Regional variation and frequency dependence of Qβ in the crust of the United States, Bull. Seismol. Soc. Am. 71 (5) (1981) 1531–1538.
[33] H. Sato, M.C. Fehler, T. Maeda, Seismic Wave Propagation and Scattering in the Earth, second ed., Springer, 2012.
[34] A. Kumar, R. Kumar, V. Ghangas, B. Sharma, MATLAB codes (CodaQ) for estimation of attenuation characteristics of coda waves, Int. J. 3 (9) (2015) 1078–1083.
[35] J. Havskov, L. Ottemoller, SEISAN earthquake analysis software, Seismol. Res. Lett. 70 (5) (1999) 532–534.
[36] K. Aki, Scattering and attenuation of shear waves in the lithosphere, J. Geophys. Res. Solid Earth 85 (B11) (1980) 6496–6504.
[37] J.J. Pulli, K. Aki, Attenuation of seismic waves in the lithosphere: comparison of active and stable areas, in: Earthquakes and Earthquake Engineering: The Eastern US, vol. 1, 1981, pp. 129–141.
[38] T.V. Eck, Attenuation of coda waves in the Dead Sea region, Bull. Seismol. Soc. Am. 78 (2) (1988) 770–779.
[39] A. Akinci, A.G. Taktak, S. Ergintav, Attenuation of coda waves in western anatolia, Phys. Earth Planet. In. 87 (1–2) (1994) 155–165.
[40] Y. Timoulali, J. Nacer, Y. Hahou, M. Chourak, Lithospheric structure in NW of Africa : case of the Moroccan atlas mountains, Geodesy Geodyn. 6 (6) (2015) 397–408.
[41] C.R.D. Woodgold, Coda Q in the Charlevoix, Quebec, region: lapse-time dependence and spatial and temporal comparisons, Bull. Seismol. Soc. Am. 84 (4) (1994) 1123–1131.
[42] E. Del Pezzo, J. Ibanez, J. Morales, A. Akinci, R. Maresca, Measurements of intrinsic and scattering seismic attenuation in the crust, Bull. Seismol. Soc. Am. 85 (5) (1995) 1373–1380.
[43] S. Mukhopadhyay, C. Tyagi, Variation of intrinsic and scattering attenuation with depth in NW Himalayas, Geophys. J. Int. 172 (3) (2008) 1055–1065.
[44] M. Ma'hood, H. Hamzehloo, G.J. Doloei, Attenuation of high frequency P and S waves in the crust of the East-Central Iran, Geophys. J. Int. 179 (3) (2009) 1669–1678.
[45] J. Havskov, S. Malone, D. McClurg, R. Crosson, Coda Q for the state of Washington, Bull. Seismol. Soc. Am. 79 (4) (1989) 1024–1038.
[46] L.B. Kvamme, J. Havskov, Q in southern Norway, Bull. Seismol. Soc. Am. 79 (5) (1989) 1575–1588.
[47] S.C. Gupta, V.N. Singh, A. Kumar, Attenuation of coda waves in the Garhwal Himalaya, India, Phys. Earth Planet. In. 87 (3–4) (1995) 247–253.
[48] S. Mukhopadhyay, C. Tyagi, Lapse time and frequency-dependent attenuation characteristics of coda waves in the Northwestern Himalayas, J. Seismol. 11 (2) (2007) 149–158.
[49] R. Kumar, S.C. Gupta, S.P. Singh, A. Kumar, The attenuation of high-frequency seismic waves in the lower Siang region of arunachal Himalaya: Qα, Qβ, Qc, Qi, and Qs, Bull. Seismol. Soc. Am. 106 (4) (2016) 1407–1422.
[50] K. Spieker, I. Wölbern, C. Thomas, M. Harnafi, L. El Moudnib, Crustal and upper-mantle structure beneath the western Atlas Mountains in SW Morocco derived from receiver functions, Geophys. J. Int. 198 (3) (2014) 1474–1485.
[51] M. Hellweg, P. Spudich, J.B. Fletcher, L.M. Baker, Stability of coda Q in the region of Parkfield, California: view from the US geological survey Parkfield dense seismograph array, J. Geophys. Res. Solid Earth 100 (B2) (1995) 2089–2102.
[52] E. Giampiccolo, S. Gresta, F. Rascona, Intrinsic and scattering attenuation from observed seismic codas in southeastern Sicily (Italy), Phys. Earth Planet. In. 145 (1–4) (2004) 55–66.
[53] H. Rahimi, H. Hamzehloo, Lapse time and frequency-dependent attenuation of coda waves in the Zagros continental collision zone in Southwestern Iran, J. Geophys. Eng. 5 (2) (2008) 173–185.
[54] S. Mukhopadhyay, J. Sharma, Attenuation characteristics of Garwhal–Kumaun Himalayas from analysis of coda of local earthquakes, J. Seismol. 4 (4) (2010) 693–713.
[55] S. Padhy, N. Subhadra, J.R. Kayal, Frequency-dependent attenuation of body and coda waves in the Andaman Sea Basin, Bull. Seismol. Soc. Am. 101 (1) (2011) 109–125.
[56] I. Shengelia, Z. Javakhishvili, N. Jorjiashvili, Coda wave attenuation for three regions of Georgia (using local earthquakes), Bull. Seismol. Soc. Am. 101 (5) (2011) 2220–2230.
[57] F. Sertçelik, Estimation of coda wave attenuation in the east Anatolia fault zone, Turkey, Pure Appl. Geophys. 169 (7) (2012) 1189–1204.
[58] S. de Lorenzo, E. Del Pezzo, F. Bianco, Q β Q c, Q i and Q s attenuation parameters in the Umbria–Marche (Italy) region, Phys. Earth Planet. In. 218 (2013) 19–30.
[59] M. Mahood, Attenuation of high-frequency seismic waves in Eastern Iran, Pure Appl. Geophys. 171 (9) (2014) 2225–2240.
[60] M. Farrokhi, H. Hamzehloo, H. Rahimi, M. Allamehzadeh, Estimation of coda-wave attenuation in the central and eastern Alborz, Iran, Bull. Seismol. Soc. Am. 105 (3) (2015) 1756–1767.
[61] H.S. Hasegawa, Attenuation of Lg waves in the Canadian shield, Bull. Seismol. Soc. Am. 75 (6) (1985) 1569–1582.
[62] L.G. Pujades, J.A. Canas, J.J. Egozcue, M.A. Puigvi, J. Gallart, X. Lana, J. Pous, A. Casas, Coda-q distribution in the Iberian Peninsula, Geophys. J. Int. 100 (2) (1990) 285–301.

[63] G.M. Atkinson, R.F. Mereu, The shape of ground motion attenuation curves in southeastern Canada, Bull. Seismol. Soc. Am. 82 (5) (1992) 2014–2031.
[64] G.M. Atkinson, Empirical attenuation of ground-motion spectral amplitudes in southeastern Canada and the northeastern United States, Bull. Seismol. Soc. Am. 94 (3) (2004) 1079–1095.
[65] C.P. Kumar, C.S.P. Sarma, M. Shekar, R.K. Chadha, Attenuation studies based on local earthquake coda waves in the southern Indian peninsular shield, Nat. Hazards 40 (3) (2007) 527–536.
[66] F. Sedaghati, S. Pezeshk, Estimation of the coda-wave attenuation and geometrical spreading in the New Madrid seismic zone, Bull. Seismol. Soc. Am. 106 (4) (2016) 1482–1498.

Roumaissae Azguet is a PhD student in seismology at Scientific Institute, Mohamed V University, Morocco. She obtained her Master Degree in Computer Science and signals treatment from faculty of science, Mohamed V University. Her research focuses on seismic waves attenuation.